JOURNAL OF EXPERIMENTAL ZOOLOGY 289:10–22 (2001)

Muscle Phenotype Remains Unaltered After Limb Autotomy and Unloading

BRUCE GRIFFIS,[1] STACIA B. MOFFETT,[2] AND ROBIN L. COOPER[1]*
[1]*Thomas Hunt Morgan School of Biological Sciences, University of Kentucky, Lexington, Kentucky 40506*
[2]*Department of Zoology, Washington State University, Pullman, Washington 99164*

ABSTRACT Loss of chelipeds in crustaceans results in severe atrophy of the major muscle responsible for lifting the limb, the anterior levator. We decided to test if this loss of mechanical load altered muscle phenotype as measured by SDS–PAGE analysis of levator total protein and actomyosin fractions. Levator muscles of adult crayfish, *Procambarus clarkii*, with either functional regenerate limbs or lack of limb buds (papilla stage) were compared with those from normal contralateral limbs and those from pristine animals. We find that there is no difference in protein profiles among the three conditions. However, the total protein profile for the dually excited levator muscle is unique compared to those of fast or slow muscles of the abdomen (L and SEL, respectively), which receive only phasic or tonic excitatory innervation. The levator myosin heavy chain profile is similar to that of slow phenotype muscles such as the SEL and opener. We conclude that load does not influence levator phenotype. This is likely due either to the intact innervation and continued activation of the levator during atrophy or to the maintenance of passive tension on the muscle. *J. Exp. Zool. 289:10–22, 2001.*

Control of phenotype in striated muscle has been shown to be dependent upon several factors. Innervation, hormones, muscle cell lineage, and load may play a role in the expression of the major contractile proteins for a particular muscle (see reviews: Pette and Vrbová, ’85, ’92, ’99; Pette and Staron, ’97). The interplay among factors is not constant for every muscle within an organism, much less across species. However, the general framework of muscle phenotype control is relatively similar for evolutionarily disparate species, for example, arthropods and vertebrates, although each factor may be weighted in a different fashion.

The major controlling influences on arthropod muscle phenotype have been examined primarily in *Drosophila* (Cripps et al., ’99; Gunthorpe et al., ’99; Jagla et al., ’99; White et al., ’99) and crustaceans (Mykles, ’97; LaFramboise et al., 2000). Investigations in *Drosophila* have revealed regulating genomic factors, such as transcription factors, including *Drosophila MyoD* (Michelson et al., ’90), S59 (Dohrmann et al., ’90), and *Dmef* and *apterous* (Bourgouin et al., ’92). However, little is known about their function in determining individual muscle fiber identity. Recently, a muscle segment homeobox (msh) gene, the homolog of vertebrate *Msxs*, has been demonstrated to be required for the specification of the precursor cells (Nose et al., ’98). Similarly, little is known about the molecular mechanisms that are responsible for regulation of muscle numbers and their insertion sites, although there is evidence that mutation of the neurogenic genes, such as *Notch* (Bate et al., ’93), and mutations of the *Spitz* class of genes, such as rhomboid (Bier et al., ’90; Chiba et al., ’93), both alter the muscle fiber number. Crustaceans, particularly crayfish, are well suited to these studies because of the vast background knowledge of their muscle innervation patterns and even of output from specific neuromuscular junctions. Muscles are easily distinguished and removed for study.

Typically, crustacean muscles have been classified according to the type of innervation each muscle receives. This leads to three broad categories of crustacean muscles: fast, slow, and mixed (or dually innervated). As their names suggest, fast and slow muscles receive only one type of excitatory input (phasic or tonic, respectively), although multiple motor neurons may innervate the

Grant sponsor: NIH-NIMH Behavioral Ecology and Comparative Neurobiology Training; Grant sponsor: National Science Foundation; Grant numbers: IBN-9808631 and ILI-OUE-9850907.

*Correspondence to: Dr. Robin L. Cooper, 100 T.H. Morgan Building, Thomas Hunt Morgan School of Biological Sciences, University of Kentucky, Lexington, Kentucky 40506-0225.
E-mail: RLCOOP1@pop.uky.edu

Received 20 March 2000; accepted 17 July 2000

same muscle. Mixed muscles receive both phasic and tonic excitation.

As with vertebrates, crustacean skeletal muscle fibers are biochemically defined on the basis of histochemical analysis that relates to a muscle's activity profile and contraction velocity (Ogonowski and Lang, '79; Mellon, '91; Günzel et al., '93; and see Mykles ('97) for review). Fast muscles primarily use glycolytic processes, whereas slow muscles primarily use oxidative metabolism. Phenotypic profiles can readily be determined by the proteins associated with particular enzymes and/or their activity. Staining profiles of ATPases have been shown to work well in crustacean muscles (Günzel et al., '93). Higher resolution of phenotypic differences in myofibrillar protein isoforms by SDS–polyacrylamide gel electrophoresis has also been successful in crustaceans (Costello and Govind, '84; Quigley and Mellon, '84; Mykles, '85a,b, '88; Neil et al., '93; Sakurai et al., '96, LaFramboise et al., 2000). One example of a particular marker for fast fibers is a 75-kDa regulatory protein (P75) (Mykles '85a,b, '88; Neil et al., '93). In addition, slow muscles have specific profiles of protein isoforms that have been used to subgroup types of slow muscles. For example, slow-tonic (S_2) fibers contain a 55-kDa isoform of troponin-T (TnT_1) not present in slow-twitch (S_1) fibers (Mykles, '85a,b, '88; Ismail and Mykles, '92; Neil et al., '93; Galler and Neil, '94). It has been shown that innervation pattern correlates with a particular protein expression pattern even at the level of myosin heavy chain (MyHC), the major contractile protein (Cotton and Mykles, '93; Galler and Neil, '94; Mykles, '97; Cooper et al., '98; LaFramboise et al., 2000).

Along with specialized innervation, crustaceans have the ability to regenerate whole limbs. This loss of limb is usually in response to life-threatening encounters with predators or conspecifics. By losing the limb, the crustacean increases its chance of surviving the encounter. This presents an ideal situation to study the effects of a "naturally" occurring event that significantly changes the load on muscles associated with limb movement (Bliss, '60).

In vertebrates, unloading of a muscle can cause an abrupt change in phenotype in a short amount of time (Talmadge et al., '96; Stevens et al., '99a,b). Unloaded muscles typically respond to the loss of load depending on their original phenotype: fast muscles stay fast while slow muscles become faster. Fibers that may once have expressed a single myosin heavy chain produce two or more isoforms of the protein. Recently, this has even been shown to produce fibers that defy the "next neighbor" rule in which vertebrate muscles switch myosin heavy chain isoforms by proceeding directly along a continuum: MyHCI > MyHC IIa > MyHC IId/x > MyHC IIb (Stevens et al., '99b).

Previous work has shown that crustacean muscles proximal to the autotomy plane atrophy after autotomy (Moffett, '87; Schmiege et al., '92). One of these muscles, the anterior levator, is responsible for the actual autotomy itself (Moffett, '75; Moffett et al., '87). Under normal conditions, the main function of the anterior levator is to lift the limbs attached to the major claws, the chelae. In the red swamp crayfish, *Procambarus clarkii*, the chelae-associated anterior levators normally have a comparatively large load during use compared to those of the walking legs, or chelipeds. Because this crayfish has bilaterally symmetrical claws, this load should be approximately equal on both sides of the animal. So, after autotomy, the anterior levator loses essentially all of its load and then regains the load as the limb regenerates. We test the question of the importance of load in determining the phenotype of the anterior levator. We used qualitative assessment of the protein isoforms separated during SDS–PAGE to identify the presence or absence of a concomitant shift in muscle phenotype with autotomy.

Parts of this study have been presented in abstract form (Griffis et al., 1999).

MATERIALS AND METHODS

Animals

Six adult (10–14 cm body length) red swamp crayfish, *P. clarkii* (Atchafalaya Biological Supply Co., Raceland, LA), including four with unilaterally autotomized chela and two with bilaterally normal chela, were used to compare protein profiles of anterior levator muscles after autotomy of one cheliped. Animals were housed in an aquatic facility and fed dried fish food.

Live weights of the intact crayfish were measured, and, after dissection, the normal and regenerate limbs (from the autotomy plane forward) were weighed. Two crayfish lacked full limb buds (papilla stage), and so this was taken as negligible weight, whereas two crayfish had small, functionally regenerate limbs (Fig. 1A,B). As another indicator of cheliped size, the length of the dorsal propus, from the carpus–propus joint to the hinge of the propus–dactylus joint, was measured for each limb (see Table 1 and Fig. 1B).

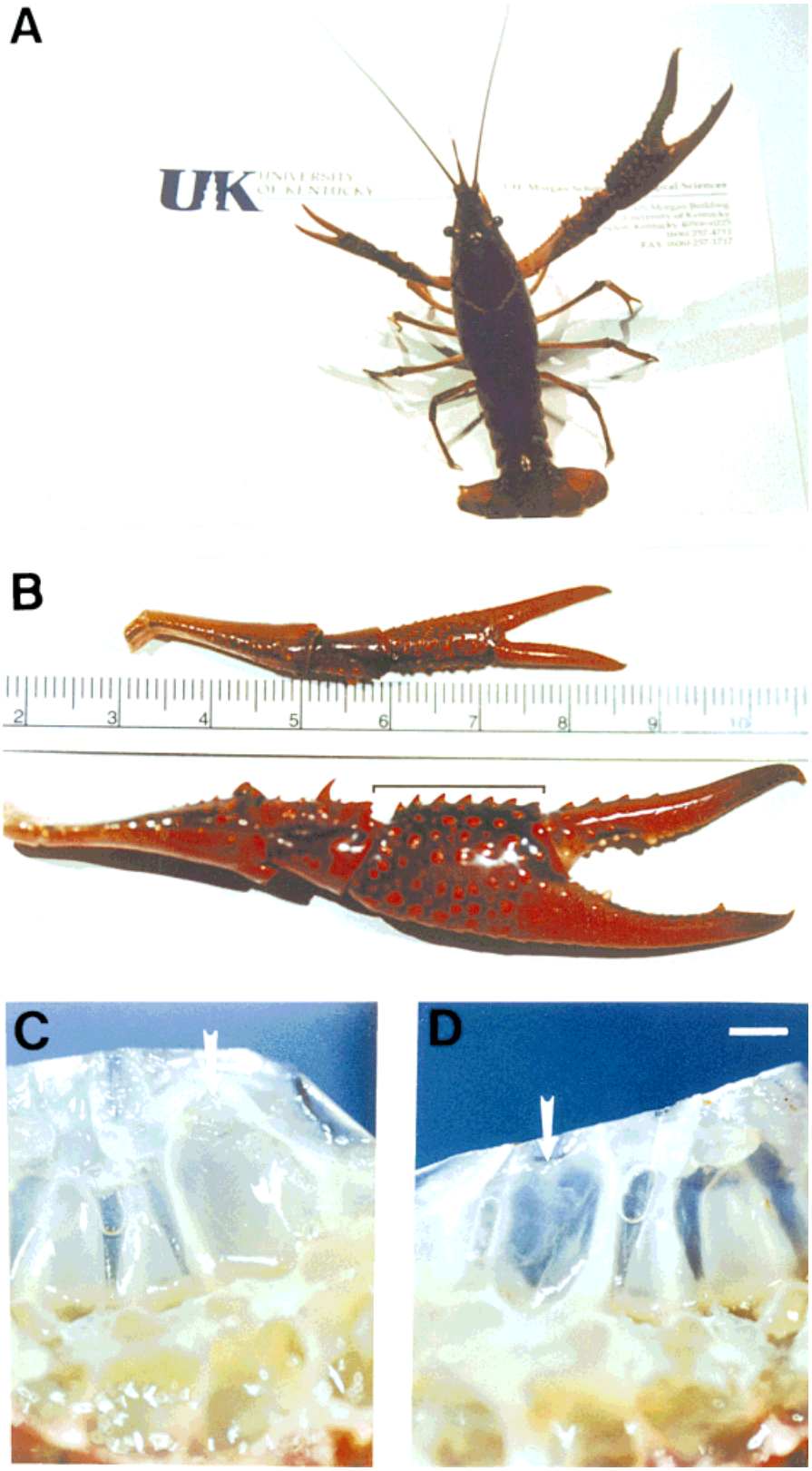

Fig. 1. Loss of the chela results in atrophy of the associated anterior levator muscle. **A:** Crayfish with a functionally regenerate chela. Difference in limb size is obvious. **B:** View of claws after removal. Bracket indicates the area measured as the dorsal propus. **C,D:** Medial view of the anterior levator muscles from a crayfish with one normal claw (C) and a papilla-stage regenerate (pre-limb bud, D). Arrows indicate the anterior levator muscles. Scale bar: 2 mm.

TABLE 1. Morphometrics and mass of the animals and their chelae

Animal	Limb	Body weight (g)	Claw weight (g)	Body weight %	Propus length (mm)	Levator weight (g)
1	Left	46.4	8.0	17.3	21	0.094
	Right		8.0	17.3	21	0.108
2	Left	31.1	4.9	15.8	17	0.060
	Right		4.9	15.8	17	0.073
3	Normal	29.0	4.4	15.2	18	0.025
	Regenerate		0.9	3.1	12	0.028
4	Normal	17.9	1.6	8.7	10	0.057
	Regenerate		0.6	3.5	7	0.038
5	Normal	30.1	6.0	19.9	19	0.043
	Papilla					0.012
6	Normal	38.4	5.4	13.9	19	0.068
	Papilla					0.028

To dissect out the anterior levator muscles, the abdomen, the gill chamber, and the walking legs were removed. The remainder of the cephalothorax was then cut in half down the ventral midline. This allowed visualization of the musculature. To be sure that the correct muscles were taken, muscle action and limb movement were correlated. Dissected preparations were maintained in crayfish saline, a modified Van Harreveld's solution (in mM: 205 NaCl; 5.3 KCl; 13.5 $CaCl_2 \cdot 2H_2O$; 2.45 $MgCl_2 \cdot 6H_2O$; 10 mM glucose; 0.5 HEPES adjusted to pH 7.4). Muscles were removed from the cuticle, with as much of the apodeme attached as possible. Muscle wet weights were recorded, and some muscles were photographed for a visual comparison of atrophy. Each muscle was cross-cut into two pieces at the muscle mid-belly: one piece used for total protein analysis, and the other was used for myosin heavy chain analysis.

Total protein analysis

The total protein fractions were immediately placed in glycerination buffer (20 mM Tris-acetate, pH 7.5, 50% glycerol, 0.1 M KCl, 1 mM EDTA, 0.1% Triton X–100) for 30 min at room temperature. Afterward, the muscles were gently pelleted by centrifugation to allow removal of the glycerination buffer and placed into 500 µl of Reagent A (0.34 g NaH_2PO_4, 1.0 g Na_2HPO_4, 1.0 ml β-mercaptoethanol, 1.0 g SDS, 0.015 g bromophenol blue, and 36.0 g urea, solution volume made up to 80 ml with ultrapure water, pH 7.0) overnight (Cooper et al., '98). Total protein samples were then analyzed by SDS–PAGE using 10% acrylamide separating gels with a 30:0.8 acrylamide/bis-acrylamide ratio, as previously described (Cooper et al., '98). One exception was that the gels were run using the Mini-PROTEAN II system (Bio-Rad, Richmond, CA) at 15 mA constant current until the dye front reached the separating gel and then at 20 mA until the dye front reached the bottom of the gel; the total run time was about 2 hr. This increased the resolution of the band separation and shortened the run time significantly (~4 hr).

Myosin heavy chain analysis

Muscle pieces for myosin extraction were placed in a –80°C freezer until the extraction procedure. Myosin heavy chain electrophoresis was performed essentially as previously described (LaFramboise et al., '90, 2000). In short, muscle was minced in 4 volumes of high-salt buffer (300 mM NaCl, 100 mM NaH_2PO_4, 50 mM Na_2HPO_4, 1 mM $MgCl_2$, 10 mM $Na_4P_2O_7$, and 10 mM EDTA; pH 6.5) and kept on ice for 30 min with frequent vortexing (Butler-Browne and Whalen, '84). The tissue was then centrifuged at 12,000*g* for 30 min at 4°C, and the supernatant was placed in 9 volumes of low-salt buffer (1 mM EDTA, 0.1% β-mercaptoethanol) overnight at 4°C. The next day, actomyosin filaments were pelleted by centrifuging for 30 min as before. The supernatant was removed, and the filaments were resuspended in myosin sample buffer (0.5 M NaCl, 10 mM NaH_2PO_4; pH 7.0) overnight at 4°C. On the third day of the extraction, the resuspended myosin was diluted with an equal volume of SDS buffer (62.5 mM Tris, 2% SDS, 10% (v/v) glycerol, 0.001% bromophenol blue, 5% β-mercaptoethanol; pH 6.8; Laemmli, '70), boiled for 2 min, and stored in a –80°C freezer. SDS–PAGE to separate myosin isoforms was performed using 5% acrylamide separating gels (28.5:1.5 acrylamide/bis-acrylamide ratio) containing 30% (v/v) glycerol. Stacking gels contained 3% acrylamide, no glycerol, and were 4.5 cm tall. Gel mixtures were completely degassed. Myosin gels were run in an SE 600 slab gel electrophoresis unit (Hoefer

Scientific Instruments) for 22 hr at 15°C. Gels were started at 120 V constant and then switched to 115 V constant when the starting amperage had decreased by ~45%. This prevented the protein bands from forming a smile across the gel.

For both gel systems, Laemmli ('70) running buffer was prepared from 10× stock just before use, with the exception that 0.1% β-mercaptoethanol was added to the upper buffer for myosin gels, as described in LaFramboise et al. (2000). Before electrophoresis, samples were boiled and diluted appropriately to ensure good separation of protein bands and to maintain good staining characteristics.

Staining and image capture

Gels were stained with Coomassie Blue R-250 in 45% methanol/10% glacial acetic acid, destained, and silver stained by the method of Wray et al. ('81) with the following modification to increase signal to noise ratio: gels were washed in 50% methanol overnight before silver staining. Stained gels were scanned with a Umax Astra 2400S scanner using Adobe Photoshop 5.0 software on a Macintosh PowerPC. After being soaked a minimum of 2 hr in 10% ethanol/7%glycerol, gels were then dried and stored with a record of run conditions.

Nerve terminal visualization

To determine the innervation pattern across the levator muscle, the dissected preparation was stained with methylene blue and photographed through a Wild dissecting microscope. This provided an initial look at the nerve terminals running across the muscle.

To identify the living nerve terminal phenotype (filiform and wispy for phasic neurons; varicosities connected by bottlenecks for tonic neurons), freshly dissected muscles were incubated for 2–5 min in 2–5 μM 4-Di-2-ASP (4-[4-(diethylamino)-styryl]-*N*-methylpyridinium iodide; Molecular Probes, Eugene, OR) in crayfish saline (Magrassi et al., '87). Following a wash with fresh saline, nerve terminals were visualized and photographed with a Nikon epifluorescence microscope using a 40× water immersion lens.

Immunofluorescence

Whole-mount preparations were pinned to a Sylgard-lined dish with the muscle in a stretched position. They were fixed with 2.5% (v/v) glutaraldehyde, 0.5% (v/v) formaldehyde dissolved in a PBS buffer (9.5 ml of 0.2 M $NaH_2PO_4 \cdot 2H_2O$, 40.5 ml of 0.2 M stock $Na_2HPO_4 \cdot 7H_2O$, 4 g sucrose, brought to 100 ml with H_2O) for 1 hr with two changes of solution at room temperature. The preparation was then placed into vials and washed in PBS buffer containing 0.2% (v/v) Triton X-100 and 1% (v/v) normal goat serum (Gibco/BRL, Grand Island, NY) for 1 hr with three changes of solution at room temperature. The tissue was then incubated with primary antibody to GABA (Sigma, 1:1,000 in PBS buffer) on a shaker at 4°C for 12 hr. Following three washes in PBS, the tissue was incubated with secondary antibody (goat, anti-rabbit IgG conjugated with Texas Red, Sigma), diluted 1:200 in PBS, at room temperature for 2 hr and washed twice with PBS. The synaptic locations were observed by immunocytochemistry as previously shown in nerve terminals (Cooper et al., '96; Cooper, '98). Fluorescent images of the nerve terminals were viewed with a Leica DM IRBE inverted fluorescent microscope using a 63× (1.2 NA) water immersion objective with appropriate illumination. The composite images of Z-series were collected with a Leica TCS NT confocal microscope for illustration.

Axon counts

The base of the nerve before reaching the levator muscle was removed in order to obtain a cross-section for observation with light and transmission electron microscopy (TEM). After the segment of nerve was cut and held in place in a Sylgard dish, the preparation was fixed in a solution containing 2.5% (v/v) glutaraldehyde and 0.5% (v/v) formaldehyde dissolved in buffer (0.1 M sodium cacodylate, 0.022% (w/v) $CaCl_2$, 4% (w/v) sucrose, adjusted to pH 7.4) for 1 hr with two changes of solution. The tissue was subsequently processed for TEM (Jahromi and Atwood, '74; Cooper, '98). The tissues for TEM were further processed after fixation by washing in PBS buffer for 2 hr, changing solution twice. Post-fixation was performed for 1 hr in 2% osmium tetroxide in buffer, followed by three rinses in PBS. The tissue was then dehydrated using a graded ethanol series (50%, 70%, 80%, 90%, 95%, 100%—3 times) and embedded in an Araldite/Epon Resin. The area of interest was sectioned and then viewed using a Hitachi H7000 electron microscope.

In order to obtain axonal measurements, thin sections of the nerve bundles were photographed at 1,500× and printed at 2.5× to form montages. The number of axons was counted, and minimum and maximum diameters of each axon were measured with a cartographer's tool. The square root

of the product of the maximum and minimum perpendicular diameters provided one measure of the mean diameter of the axon. The other was calculated from the measured perimeter of the axon.

RESULTS

Levator weight relative to limb weight

The gross morphology and location of the anterior levator muscle is shown in Fig. 1C and D. In Fig. 1D, the ability of the muscle to undergo extreme atrophy is shown. Table 1 provides the wet weights of anterior levator muscles for animals with normal chelae and for those that had undergone autotomy. Two animals had the presence of limb buds at the stage in which the individual leg segments could be discerned and the two other animals only had a papilla, an early stage of limb regeneration (Cooper, '98). In one of the regenerative cases, the cheliped from the autotomized side was in an advanced stage of regeneration and had likely experienced two full molt cycles. The levator for this advanced stage regenerate had nearly undergone a full recovery in mass, as compared to the contralateral control side. As indicated in Table 1, larger animals had larger chelae and also larger levator muscles. The animals with one cheliped missing for at least a month, as determined by the presence of the small papilla (Cooper, '98), experienced a massive reduction in mass. In contrast, the one with a substantially regenerated limb had regained most of its muscle mass.

Anatomy

Methylene blue staining of the anterior levator is shown in Fig. 2A, with the anatomy more clearly defined in the accompanying drawing (Fig. 2B). The staining revealed that the nerve to the levator muscle arrives at the base and travels dorsally along the medial half of the muscle. A branch of the nerve, close to the point of arrival on the levator, takes a route through the levator fibers to arise on the other surface (lateral) of the levator between the levator and the more lateral remoter muscle. This is illustrated by the small line in Fig. 2B. This branch continues along to a more caudal aspect of the levator and additional branching occurs on the caudal, dorsal region of the levator.

The fine terminals of the neurons are easily seen with the 4— Di— 2–ASP staining (Fig. 2D,E). There are multiple terminals with varicosities found on all regions sampled on the medial surface of the muscle. We sampled along the base, middle, and dorsal groups of fibers. The presence of varicose terminals indicates that they are tonic in nature. We also observed fine filiform terminals indicative of phasic motor neurons.

Immunohistochemistry with an antibody against GABA (γ-aminobutyric acid) revealed immunoreactivity in some of the varicosities, indicating that the inhibitory innervation to this muscle is also tonic in nature (Fig. 2C). This inhibitory innervation correlates with that seen to the anterior levator of crabs (Moffett and Yox, '86).

Axon counts

The cross-section of the nerve bundle located at the base of the anterior levator revealed a range of axon diameters (Fig. 3). Axons diameters are given in Table 2. Some axons, indicated by the bracket, could not be measured. From the measurements that were made, at least eleven separate motor neurons innervate the anterior levator muscle in these crayfish. This is probably an underestimation; however, we have chosen to be conservative since the smaller nerve bundle could be a branch of the larger. As can be seen in Table 2, the measured axonal diameter depends upon the method of measurement. The two methods, square root and perimeter, only give measurements in close agreement for a few axons. These variances

TABLE 2. Axon profiles of the innervating nerve

Large bundle axon	Square root method (μm)	Perimeter method (μm)	Small bundle axon	Square root method (μm)	Perimeter method (μm)
1	98.29	89.54	1	9.62	6.85
2	41.18	46.22	2	13.56	9.75
3	9.48	10.84	3	7.85	5.76
4	6.40	6.49	4	5.53	4.31
5	23.18	24.54	5	18.28	18.78
6	32.48	35.39	6	4.54	3.27
7	68.04	73.61	7	6.80	3.63
8	30.43	29.62	8	3.95	2.90
9	16.06	14.79	9	9.07	7.57
10	51.98	49.08	10	4.54	2.90
11	24.72	25.26			

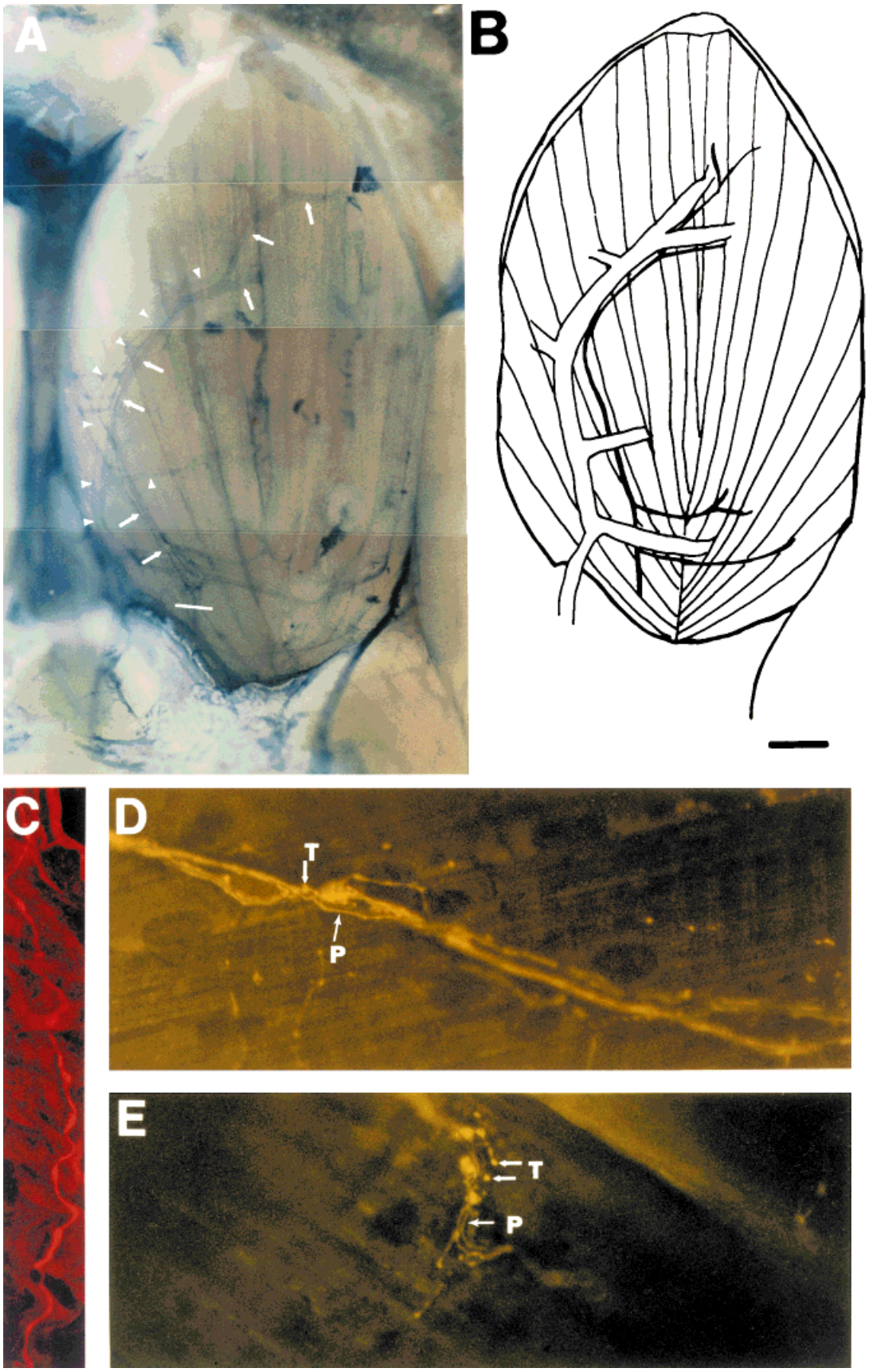

Figure 2.

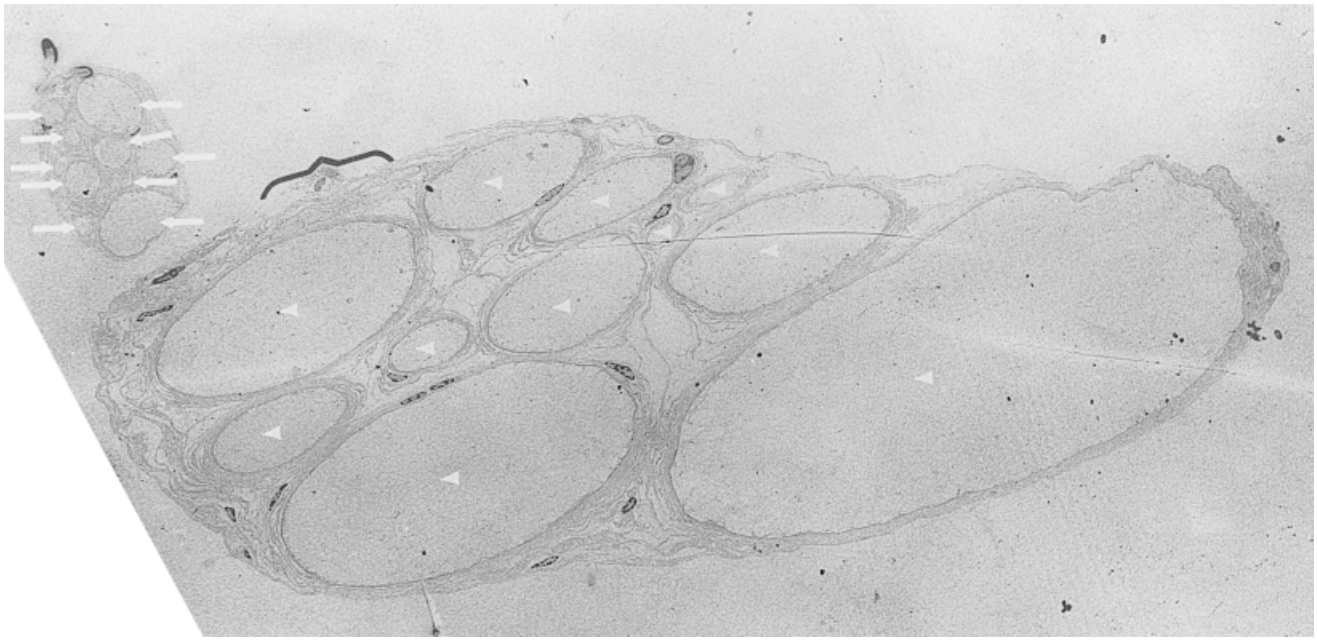

Fig. 3. Cross-section of the anterior levator associated nerve bundle. Section taken before the bifurcation along the ventral portion of the muscle. Arrows and triangles indicate individual axons. The bracket indicates a region of very small axon branches. The sizes of the axonal diameters measured by perimeter and perpendicular diameters square root methods are shown in Table 2.

are likely due to the invaginations of some of the membranes as well as the angle of the cross-section, i.e., the cross-sections were not perfectly perpendicular to the axon.

Myofibrillar proteins

The protein banding pattern revealed by 10% SDS–polyacrylamide gels consistently shows unique profiles for the levator as compared to control tonic and phasic muscles. As seen in Fig. 4A, the two control muscles, L_1 (fast) and SEL (slow), extensor muscles from the dorsal abdomen of these crayfish, have distinct protein-banding profiles. Likewise, the anterior levator muscle profiles, from control and atrophied muscles, are distinctly different from the L_1 and SEL controls (Fig. 4B). The protein bands that appear at the top of the gels are myosin heavy chains. The next smaller bands, between 100 and 140 kDa, are various paramyosin isoforms, as reported in lobster fast and slow muscles by Mykles (’85) and in crayfish muscles (Cooper et al., ’98). Previous identification of the other bands in the profiles is provided in Cooper et al. (’98) with the exception that the P75 band was previously mislabeled as 85 kDa for L_1 muscle.

The anterior levator from control and autotomized sides of the animal did not show any differences in banding pattern (Fig. 4B). They did exhibit bands not present in either of the two control abdominal muscles, again reinforcing the idea that the anterior levator is a mixed-phenotype muscle.

The myosin expression in the levator is similar to that seen for slow muscles (Fig. 5), with the same three bands present but in different proportions compared with slow SEL muscle. We detected no myosin isoform alterations in muscles with extreme atrophy or rebuilding associated with autotomy. The three myosin bands present have been previously identified as C1, C3, and C4 (LaFramboise et al., 2000). The large amount of the fastest migrating band, C1, compared with the slow SEL indicates that while the anterior levator exhibits a slow myosin phenotype, it is more

Fig. 2. Innervation pattern and anatomy of the anterior levator muscle associated with the chela. **A:** Methylene blue stained anterior levator muscle. Triangles point to the blood vessel associated with the nerve bundle (arrows). **B:** Tracing of the stained levator in A to more clearly depict the innervation. The most ventral portion of the levator is innervated by a branch of the nerve that bifurcates near the base of the muscle. **C:** Anti-GABA staining demonstrated the innervation of the levator by a GABAergic neuron that has varicose terminals. **D,E:** Staining of the nerve terminals with 4-Di-2-ASP revealed both phasic (P, filiform) and tonic (T, varicose) terminals. Scale bar: A/B, 0.6 mm.

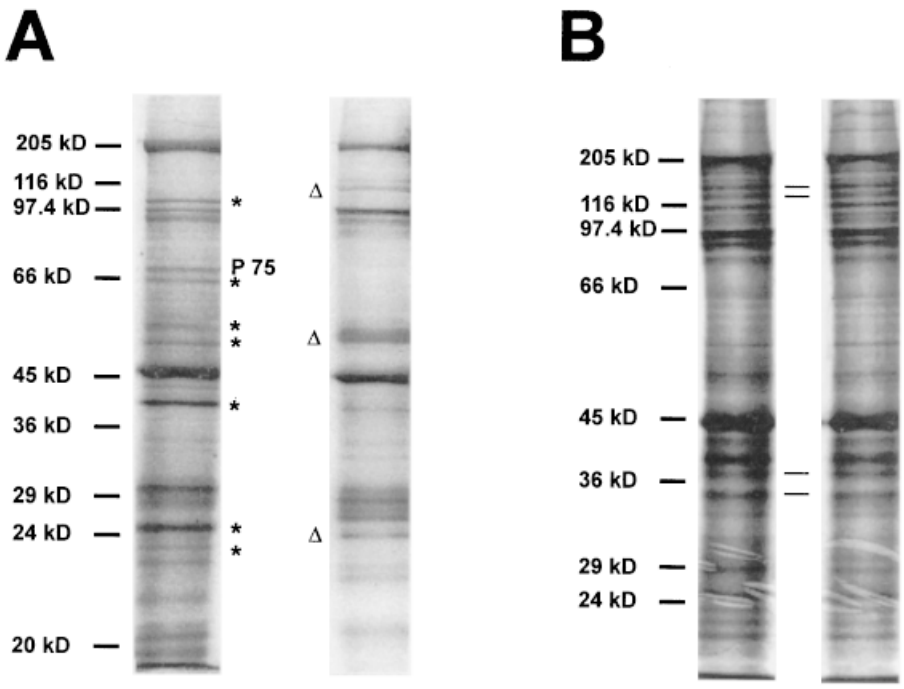

Fig. 4. SDS–PAGE of total protein fractions reveals a unique phenotype for the anterior levator. **A:** Purely phasic L muscle (left band) and purely tonic SEL muscle (right band) with unique protein bands indicated. **B:** Control (left band) and atrophied (right band) levator show no differences. Possible unique protein bands are indicated.

similar to the opener muscle than to the SEL (LaFramboise et al., 2000).

DISCUSSION

We have shown in this study that the anterior levator of the chela-associated limb in the red swamp crayfish consists of a mixed biochemical phenotype. The myofibers contain proteins that are common to both slow and fast fibers. This fits with the fact that both tonic and phasic motor nerve innervation is anatomically observed. In addition, the results demonstrate that this muscle undergoes a substantial reduction in mass following autotomy. As the limb regenerates, the muscle regains its mass. Despite the atrophy and regrowth associated with limb loss and regeneration, the anterior levator muscle does not alter its biochemical phenotype. These findings illustrate that a mixed-phenotype muscle does not alter its ratio of phasic to tonic expression of proteins during large changes in the muscle's load and mass.

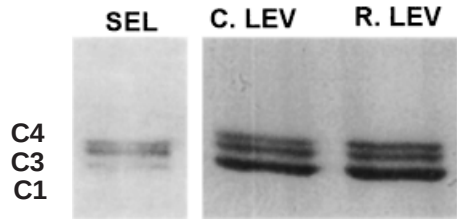

Fig. 5. SDS–PAGE of myosin heavy chain indicates anterior levator contains three myosin isoforms. The isoforms are the same as in the purely tonic SEL muscle but are in different proportions. Again, no differences were observed between control or atrophied levator.

This result is in contrast to the changes reported for vertebrate muscles. Vertebrate muscle studies show that unloading of slow muscles results in transformation to a faster muscle phenotype [see review by Pette and Staron, '97]. Like the anterior levator of the crayfish, the soleus muscle of vertebrates is of mixed phenotype, containing both slow and fast fibers, although individual muscle fibers in vertebrates receive only tonic or phasic innervation. Similar questions of muscle phenotype control are being addressed using the soleus. Unloading of the soleus revealed that there is substantial switching of slow fibers to fast fibers. A more detailed study of motor units (Leterme and Falempin, '96) concluded that the newly appearing fast fibers arose from slow–intermediate fibers. Intriguing studies in which rats have been exposed to weightlessness (space flight) demonstrated that slow muscles show a transformation to a faster phenotype, in both their myosin heavy chain composition and reduction of

myonuclei of slow fibers (Allen et al., '96; Talmadge et al., '96). However, fast muscle fibers did not show phenotype switching with unloading (Allen et al., '96; Talmadge et al., '96). Hence, the direction of transformation with unloading appears to work only in the slow to fast direction.

Another approach used to decrease muscle activity has been to transect the motor nerve. Following denervation, vertebrate motor nerve terminals degrade and are removed. There is a large body of research in vertebrates using denervation to alter phenotype (see review by Pette and Staron, '97). In short, muscle phenotype transformation appears to be muscle-type and organism dependent. The rabbit gastrocnemius became more slow-like following denervation (d'Albis et al., '95). In rats, transformation is region specific within the slow soleus and fast plantaris muscles in which individual fibers show transformation from a fast type to a slow type with denervation (Sakuma et al., '97). As with unloading paradigms, the results of phenotype switching vary depending on the muscle, although the general theme is that slow muscles become faster with unloading but fast muscles do not change phenotype while denervated muscles generally shift in the opposite direction from their starting point—from fast to slow or vice versa. However, in crustaceans, the intact nerve terminals are viable up to a year and can still convey signals through spontaneous release of substances and/or through direct membrane contact which may influence the muscle state (Atwood et al., '89; Parnas et al., '91).

Most studies of muscle phenotype transformation have focused on specific proteins that regulate the speed of contraction. By examination of the distribution of the various myosin isoforms (Hämäläinen and Pette, '96; Jürimäe et al., '96; Okumoto et al., '96) or other proteins, such as the sarcoplasmic reticulum Ca^{2+} ATPase (Nozais et al., '96), factors controlling the functional phenotype have been elucidated for many muscles. In human quadriceps muscle, removal of load does not cause any alteration in myosin heavy chain isoforms but does induce changes in the myosin light chain expression (Larsson et al., '96).

In contrast to manipulating loss of function by unloading and denervation, stimulation of nerves reveals the capacity of muscle to respond to different patterns of activity. Chronic low-frequency stimulation can result in a fast-to-slow phenotype transformation of mammalian skeletal muscles [Delp and Pette, '94; see review by Pette and Vrbová, '92; Pette and Vrbová, '99]. This alteration of phenotype can also be accomplished in the other direction (Hämäläinen and Pette, '96). Activity is likely the main mechanism responsible for transformation during development, although factors like hormones certainly play a role. This has been shown in crustaceans as well, with the control of the dimorphism of the claws of the snapping shrimp and the American lobster (Lang et al., '77; Govind, '84; Quigley and Mellon, '84).

Muscle phenotyping in crustaceans has largely been descriptive, allowing comparisons with vertebrate homologs (Mykles, '85b; Govind et al., '87; LaFramboise et al., 2000). Developmental changes in muscle phenotype associated with particular functions are well described in the cutter and crusher chelae of lobsters and the pincer and snapper chelae of snapping shrimp (Govind et al., '87). This is also recapitulated during limb regeneration in which the muscle follows its ontogenetic program (Govind, '84). Chronic stimulation of crustacean motor nerves has shown that the nerve terminals of phasic neurons are transformed to a tonic-like state (Lnenicka and Atwood, '85; Mercier and Atwood, '89; Bradacs et al., '90; Cooper et al., '98) and that, like vertebrate models, the fast muscles transform to a slow-like phenotype (Cooper et al., '98). The muscle transformation takes considerably longer than that of the nerve, and the exact protein isoforms that do transform remain to be determined.

As far as we are aware, unloading of crustacean muscles has not been used to examine muscle phenotype transformation. Because it was previously shown that some muscles proximal to the autotomy plane undergo massive atrophy with the loss of their associated limb (Moffett, '87), we chose to examine whether a phenotype transformation might be associated with the atrophy and rebuilding of the anterior levator muscle as its associated limb regenerated. The results of this study indicate for the anterior levator that no phenotype transformation occurs, whereas muscles in vertebrates that show disuse atrophy alter their phenotype (Jakubiec-Puka, '92, '99; Eller, '99). This lack of phenotype switch may reflect the lack of a load-regulated capacity to alter phenotype. The fact that these crayfish have bilaterally symmetrical claws means that any alteration would be likely short-lived as the chelipeds will eventually be of similar size. Therefore, this lack of switching may indicate that it is less energetically costly for the anterior levator muscle in crustaceans to not undergo a phenotype change during the unloaded period than to do so and change

back to its original state after the ontogenetic program has regenerated the limb. This is, of course, speculation because other muscles within crustaceans have not been examined during natural or experimentally induced unloading and reloading. Physical characteristics that may prevent phenotype switching in the unloaded anterior levator are the maintained presence of the motor nerve terminals or passive tension maintained by the cuticular attachments. These two characteristics have been shown to prevent switching of myosin isoforms in rats but not to prevent the atrophy due to lack of load (Leterme and Falempin, '94; Leterme et al., '94).

The act of molting in crustaceans also results in atrophy and post-molt rebuilding of some muscles, in particular those that are in the chelae (Mykles and Skinner, '81, '82a,b). The atrophy has been shown to be regulated by Ca^{2+}-dependent proteinases which degrade myofibrillar proteins, such as actin, troponin, tropomyosin, and myosin (Mykles and Skinner, '82b; Beyette and Mykles, '92). In these cases, widespread phenotype transformation does not appear to take place, probably for the same reasons as for the anterior levator in that during the post-molt rebuilding phase the myofibrillar apparatus needs to quickly assemble and each muscle still maintains its original function. However, in the developing claws of lobsters, new fast or new slow fibers appear, likely due to phenotype switching of existing "intermediate" fibers (Govind, '84).

The experimental manipulations described in this study will allow further investigation of plasticity among muscles under controlled laboratory conditions that are related to the animal's natural environment. Further studies may allow the similarities and differences in the control of muscle phenotype between vertebrate and invertebrate species to be more precisely defined.

ACKNOWLEDGMENTS

Funding was provided by a NIH-NIMH Behavioral Ecology and Comparative Neurobiology Training Grant to B.P.G and by NSF Grants IBN-9808631 and ILI-DUE-9850907 to R.L.C.

LITERATURE CITED

Allen DL, Yasui W, Tanaka T, Ohira Y, Nagaoka S, Sekiguchi C, Hinds WE, Roy RR, Edgerton VR. 1996. Myonuclear number and myosin heavy chain expression in rat soleus single muscle fibers after space flight. J Appl Physiol 81:145–151.

Atwood HL, Dudel J, Feinstein N, Parnas I. 1989. Long-term survival of decentralized axons and incorporation of satellite cells in motor neurons of rock lobsters. Neurosci Lett 101:121–126.

Bate M, Rushton E, Frasch M. 1993. A dual requirement for neurogenic genes in *Drosophila myogenesis*. Development (Suppl) 149–161.

Beyette JR, Mykles DL. 1992. Immunocytochemical localization of the multicatalytic proteinase (proteasome) in crustacean striated muscles. Muscle Nerve 15:1023–1035.

Bier E, Jan LY, Jan YN. 1990. *rhomboid*, a gene required for dorso–ventral axis establishment and peripheral nerve system development in *Drosophila melanogaster*. Genes Dev 4:190–203.

Bliss, D.E. 1960. Autotomy and regeneration. In: Waterman, TH, editor. The physiology of crustacea, vol. I, Metabolism and growth. New York: Academic Press. p 561–589.

Bourgouin C, Lundgrin SE, Thomas JB. 1992. *apterous* is a *Drosophila* LIM domain gene required for the development of subset of embryonic muscles. Neuron 9:549–561.

Bradacs H, Mercier AJ, Atwood HL. 1990. Long-term adaptation in lobster motor neurons and compensation of transmitter release by synergistic inputs. Neurosci Lett 108: 110–115.

Butler-Browne GS, Whalen RG. 1984. Myosin isozyme transitions during the postnatal development of the rat soleus muscle. Dev Biol 102:324–334.

Chiba A, Hing H, Cash S, Keshishian H. 1993. Growth cone choices of *Drosophila* motoneurons in response to muscle fiber mismatch. J Neurosci 13:714–732.

Cooper RL. 1998. Development of sensory processes during limb regeneration in adult crayfish. J Exp Biol 201:1745–1752.

Cooper RL, Harrington CC, Marin L, Atwood HL. 1996. Quantal release at visualized terminals of a crayfish motor axon: intraterminal and regional differences. J Comp Neurol 375:583–600.

Cooper RL, Warren WM, Ashby HE. 1998. Activity of phasic motor neurons partially transforms the neuronal and muscle phenotype to a tonic-like state. Muscle Nerve 21:921–931.

Costello WJ, Govind CK. 1984. Contractile proteins of fast and slow fibers during differentiation of lobster claw muscle. Dev Biol 104:434–440.

Cotton JLS, Mykles DL. 1993. Cloning of a crustacean myosin heavy chain isoform: exclusive expression in fast muscle. J Exp Zool 267:578–586.

Cripps RM, Zhao B, Olson EN. 1999. Transcription of the myogenic regulatory gene Mef2 in cardiac, somatic, and visceral muscle cell lineages is regulated by a Tinman-dependent core enhancer. Dev Biol 215:420–430.

d'Albis A, Couteaux R, Goubel F, Janmot C, Mira JC. 1995. Relationship between muscle myosin isoforms and contractile features in rabbit fast-twitch denervated muscle. FEBS Lett 375:67–68.

Delp MD, Pette D. 1994. Morphological changes during fiber type transitions in low— frequency— stimulated rat fast— twitch muscle. Cell Tissue Res 277:363–371.

Dohrmann C, Azpiazu N, Frasch M. 1990. A new *Drosophila* homeobox gene is expressed in mesodermal precursor cells of distinct muscle fibers during embryogenesis. Genes Dev 4:2098–2111.

Eller A, Pintsaar A, Rohtlaan EM, Gapejeva J. 1999. Changes in functional characteristics and myosin heavy chain composition in m. vastus medialis before and after arthroscopy for knee injury. Knee Surg Sports Traumatol Arthrosc 7:107–110.

Galler S, Neil DM. 1994. Calcium-activated and stretch-in-

duced force responses in two biochemically defined muscle fibre types of the Norway lobster. J Muscle Res Cell Motil 15:390–399.
Govind CK. 1984. Development of asymmetry in the neuromuscular system of lobster claws. Biol Bull167:94–119.
Govind CK, Mellon DeF Jr, Quigley MM. 1987. Muscle and muscle fiber type transformation in clawed crustaceans. Am Zool 27:1079–1098.
Griffis B, Moffett S, Cooper RL. 1999. Load does not influence muscle phenotype in crayfish. Am Zool 39:42A.
Gunthorpe D, Beatty KE, Taylor MV. 1999. Different levels, but not different isoforms, of the *Drosophila* transcription factor DMEF2 affect distinct aspects of muscle differentiation. Dev Biol 215:130–145.
Günzel D, Galler S, Rathmayer W. 1993. Fibre heterogeneity in the closer and opener muscles of the crayfish walking legs. J Exp Biol 175:267–281.
Hämäläinen N, Pette D. 1996. Slow-to-fast transitions in myosin expression of rat soleus muscle by phasic high-frequency stimulation. FEBS Lett 399:220–222.
Ismail SZM, Mykles DL. 1992. Differential molt-induced atrophy in the dimorphic claws of male fiddler crabs, *Uca pugnax*. J Exp Zool 263:18–31.
Jagla T, Bellard F, Vonesch JL, Bellard M, Dastugue B, Jagla K. 1999. Plasticity within the lateral somatic mesoderm of *Drosophila* embryos. Int J Dev Biol 43:571–573.
Jahromi SS, Atwood HL. 1974. Three-dimensional ultrastructure of the crayfish neuromuscular apparatus. J Cell Biol 63:599–613.
Jakubiec-Puka A, Catani C, Carraro U. 1992. Myosin heavy chain composition in striated muscle after tenotomy. Biochem J 282:237–242.
Jakubiec-Puka A, Ciechomska I, Morga J, Matusiak A. 1999. Contents of myosin heavy chains in denervated slow and fast rat leg muscles. Comp Biochem Physiol B: Biochem Mol Biol 122:355–362.
Jürimäe J, Abernethy PJ, Blake K, McEniery MT. 1996. Changes in the myosin heavy chain isoform profile of the triceps brachii muscle following 12 weeks of resistance training. Eur J Appl Physiol 74:287–292.
Laemmli UK. 1970. Cleavage of structural proteins during the assembly of the head of bacteriophage T4. Nature 227: 680–685.
LaFramboise WA, Daood MJ, Guthrie RD, Moretti P, Schiaffino S, Ontell M. 1990. Electrophoretic separation and immunological identification of type 2× myosin heavy chain in rat skeletal muscle. Biochim Biophys Acta 1035:109–112.
LaFramboise WA, Griffis B, Bonner P, Warren W, Scalise D, Guthrie RD, Cooper RL. 2000. Muscle type-specific myosin isoforms in crustacean muscles. J Exp Zool 286:36–48.
Lang F, Costello WJ, Govind CK. 1977. Development of the dimorphic claw closer muscles of the lobster *Homarus americanus*. I. Regional distribution of muscle fiber types in adults. Biol Bull 152:75–83.
Larsson L, Li X, Berg HE, Frontera WR. 1996. Effects of removal of weight-bearing function on contractility and myosin isoform composition in single human skeletal muscle cells. Pfluegers Arch 432:320–328.
Leterme D, Falempin M. 1994. Compensatory effects of chronic electrostimulation on unweighted rat soleus muscle. Pfluegers Arch 426:155–160.
Leterme D, Falempin M. 1996. Contractile properties of rat soleus motor units following 14 days of hindlimb unloading. Pfluegers Arch 432:313–319.
Leterme D, Cordonnier C, Mounier Y, Falempin M. 1994. Influence of chronic stretching upon rat soleus muscle during non-weight-bearing conditions. Pfluegers Arch 429:274–279.
Lnenicka GA, Atwood HL. 1985. Long-term facilitation and long-term adaptation at synapses of a crayfish phasic motoneuron. J Neurobiol 16:97–110.
Magrassi L, Purves D, Lichtman JW. 1987. Fluorescent probes that stain living nerve terminals. J Neurosci 7:1207–1214.
Mellon DeF Jr. 1991. Connective tissue and supporting structures. In: Harrison FW, Humes AG, editors. Microscopic anatomy of invertebrates, vol. 10, Decapod Crustacea. New York: John Wiley and Sons, Inc. p 77–116.
Mercier AJ, Atwood HL. 1989. Long-term adaptation of a phasic extensor motoneuron in crayfish. J Exp Biol 145:9–22.
Michelson AM, Abmayr SM, Bate M, Martinez Arias A, Maniatis T. 1990. Expression of MyoD family member prefigures muscle pattern in *Drosophila* embryos. Genes Dev 4:2086–2097.
Moffet SB. 1975. Motor patterns and structural interactions of the basi-ischiopodite levator muscles in routine limb elevation and production of autotomy in the land crab, *Cardisoma guanhumi*. J Comp Physiol 96:285–305.
Moffett SB. 1987. Muscles proximal to the fracture plane atrophy after limb autotomy in decapod crustaceans. J Exp Zool 244:485–490.
Moffett SB, Yox DP. 1986. The common inhibitor innervates muscles proximal to the autotomy fracture plane in *Carcinus maenas*. Brain Res 366:388–391.
Moffet SB, Yox DP, Kahan LB, Ridgway LB. 1987. Innervation of the anterior and posterior levator muscles of the fifth leg of the crab *Carcinus maenas*. J Exp Biol 127:229–248.
Mykles DL. 1985a. Multiple variants of myofibrillar proteins in single fibers of lobster claw muscles: evidence for two types of slow fibers in the cutter closer muscle. Biol Bull 169:476–483.
Mykles DL. 1985b. Heterogeneity of myofibrillar proteins in lobster fast and slow muscles: variants of troponin, paramyosin, and myosin light chains comprise four distinct protein assemblages. J Exp Zool 234:23–32.
Mykles DL. 1988. Histochemical and biochemical characterization of two slow fiber types in decapod crustacean muscles. J Exp Zool 245:232–243.
Mykles DL. 1997. Crustacean muscle plasticity: molecular mechanisms determining mass and contractile properties. Comp Biochem Physiol 117B:367–378.
Mykles DL, Skinner DM. 1981. Preferential loss of thin filaments during molt-induced atrophy in crab claw muscle. J Ultrastruct Res 75:314–325.
Mykles DL, Skinner DM. 1982a. Crustacean muscles: atrophy and regeneration during molting. Soc Gen Physiol Ser 37:337–357.
Mykles DL, Skinner DM. 1982b. Molt cycle-associated changes in calcium-dependent proteinase activity that degrades actin and myosin in crustacean muscle. Dev Biol 92:386–397.
Neil DM, Fowler WS, Tobasnick G. 1993. Myofibrillar protein composition correlates with histochemistry in fibres of the abdominal flexor muscles of the Norway lobster *Nephrops norvegicus*. J Exp Biol 183:185–201.
Nose A, Isshiki T, Takeichi M. 1998. Regional specification of muscle progenitors in *Drosophila*: the role of the msh homeobox gene. Development 125:215–223.
Nozais M, Lompre AM, Janmot C, d'Albis A. 1996. Sarco(endo)-plasmic reticulum Ca^{2+} pump and metabolic enzyme expression in rabbit fast-type and slow-type denervated skeletal muscles. A time course study. Eur J Biochem 238:807–812.
Ogonowski MM, Lang F. 1979. Histochemical evidence for

enzyme differences in crustacean fast and slow muscle. J Exp Zool 207:143–151.

Okumoto T, Imoto T, Katsuta S, Wada M. 1996. Severe endurance training fails to change myosin heavy-chain distribution of diaphragm. Resp Physiol 104:39–43.

Parnas I, Dudel J, Atwood HL. 1991. Synaptic transmission in decentralized axons of rock lobster. J Neurosci 11:1309–1315.

Pette D, Staron RS. 1997. Mammalian skeletal muscle fiber type transitions. Int Rev Cytol 170:143–223.

Pette D, Vrbová G. 1985. Invited review: Neural control of phenotypic expression in mammalian muscle fibers. Muscle Nerve 8:676–689.

Pette D, Vrbová G. 1992. Adaptation of mammalian skeletal muscle fibers to chronic electrical stimulation. Rev Physiol Biochem Pharmacol 120:115–202.

Pette D, Vrbová G. 1999. What does chronic electrical stimulation teach us about muscle plasticity? Muscle Nerve 22:666–677.

Quigley MM, Mellon DeF Jr. 1984. Changes in myofibrillar gene expression during fiber-type transformation in the claw closer muscles of the snapping shrimp, *Alpheus heterochelis*. Dev Biol 106:262–265.

Sakuma K, Saitoh A, Katsuta S. 1997. Denervation-induced region-specific changes in fibre types in the soleus and plantaris muscles of rats. Acta Neuropathol (Berlin) 93:129–135.

Sakurai Y, Kanzawa N, Maruyama K. 1996. Characterization of myosin and paramyosin from crayfish fast and slow muscles. Comp Biochem Physiol 113B:105–111.

Schmiege DL, Ridgway RL, Moffett SB. 1992. Ultrastructure of autotomy-induced atrophy of muscles in the crab *Carcinus maenas*. Can J Zool 70:841–851.

Stevens L, Gohlsch B, Mounier Y, Pette D. 1999a. Changes in myosin heavy chain mRNA and protein isoforms in single fibers of unloaded rat soleus muscle. FEBS Lett 463:15–18.

Stevens L, Sultan KR, Peuker H, Gohlsch B, Mounier Y, Pette D. 1999b. Time-dependent changes in myosin heavy chain mRNA and protein isoforms in unloaded soleus muscle of rat. Am J Physiol 277:C1044–1049.

Talmadge RJ, Roy RR, Edgerton VR. 1996. Distribution of myosin heavy chain isoforms in non-weight-bearing rat soleus muscle fibers. J Appl Physiol 81:2540–2546.

White KP, Rifkin SA, Hurban P, Hogness DS. 1999. Microarray analysis of *Drosophila* development during metamorphosis. Science 286:2179–2184.

Wray W, Boulikas T, Wray VP, Hancock R. 1981. Silver staining of proteins in polyacrylamide gels. Anal Biochem 118: 197–203.